2022

On the Feasibility of Model-Based Design and Optimal Control of Industrial Air-Conditioning System

Noma Park

Han Won Park

Soo Kyung Kim

Zhe Quan Jin

Hyuk Min Kwon

See next page for additional authors

Authors
Noma Park, Han Won Park, Soo Kyung Kim, Zhe Quan Jin, Hyuk Min Kwon, Jin Min Cho, Yoon Jei Hwang, and Sai Kee Oh

On the Feasibility of Model-Based Design and Optimal Control of Industrial Air-Conditioning System

Noma PARK[1]*, Hanwon PARK[1], Sookyung KIM[1], Zhe Quan JIN[1], Hyukmin KWON[1], Jin Min CHO[1], Yoonjei HWANG[1], Saikee OH[1]

[1]H&A R&D Center, Home Appliance & Air Solution Company, LG Electronics,
51 Gasan Digital 1-Ro, Geumcheon Gu, Seoul, 08592, Republic of Korea
Phone: 82-10-7584-5666, e-Mail: noma.park@lge.com

* Corresponding Author

ABSTRACT

This paper concerns the model-based design (MBD) of air-handling unit (AHU) based industrial air conditioning system and its optimal control strategy. It also addresses on why MBD is the best way of overcoming difficulty and complexity in the development of industrial air-conditioning systems by means of field tests or experiments in a psychrometric chamber. In this work, numerical models of AHU components including condensing unit (CDU), heat exchanger coils, desiccant wheels, are integrated to be a hardware-in-the-loop simulation (HILS) system incorporated with a controller hardware. The HILS system constructs a virtual replica, or a digital twin of the AHU system of a battery-separator-film manufacturing factory, the reference site. Validated against measurement data at the reference site, developed virtual system is applied to derive the optimal control strategy for the target evaporating pressures of CDUs with variable speed compressors. For all possible outdoor and return air conditions, candidates of target evaporating pressures are evaluated and weighted under the concept of reinforced learning toward minimal energy cost. It is expected that the best control strategy leads to yearly running cost saving up to 45% as compared to the current simple rule-based control strategy, which leads to 2.9-year payback period for the inverter based CDU systems. The present research demonstrates a digital twin can be a powerful tool to derive the optimal control strategy and achieve maximum energy cost savings for industrial AC systems.

1. INTRODUCTION

Unlike residential air-conditioning system whose main concern is the thermal comfort of residents, industrial air-conditioning (IAC) aims at maintaining desired air conditions for non-residential purposes such as medical operations, data centers, experimental laboratories, and manufacturing of various products including semi-conductors, electronic devices, batteries, foods, bio-chemical products, and so on. In most applications, IAC requires precise temperature and humidity control with small tolerable margin, which is typically less than 0.5ºC regardless of outdoor weather condition. In addition, some applications require special level of cleanliness and/or air-pressure control.

Toward these ends, the air-handling unit (AHUs) as shown in Fig. 1 is introduced as the key element of IAC, which integrates various ducts, fans, filters, rotors and coils to meet desired supply air condition. All these individual devices are typically connected to DDCs (direct digital controllers), all-in-one controllers, in order to operate each of them under control of the main algorithm. Sensor data collected at DDC is transferred to a server and usually monitored at the control room by the facility manager.

Korean domestic market size for IAC is rapidly growing, and is about 400 million USD in 2021. The global market size is assumed to be at least 20 billion USD, which is estimated from 6 billion USD, the gross revenue of major Japanese industrial AC companies in 2019. Thus, global residential AC companies are trying to expand their business area toward IAC.

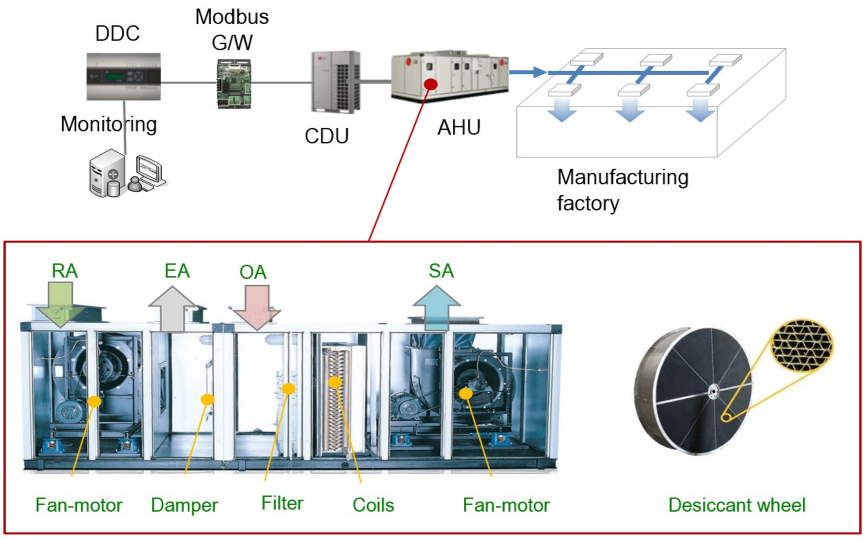

Figure 1: Industrial air-conditioning system and components of air-handling unit

Most residential AC companies, however, are having difficulties in penetrating the industrial AC market. They suffer from 'on-demand' and 'on-site' nature of the IAC systems whose design is entirely dependent upon the specific requirements of the site and clients. Ordering a new HVAC system, the clients consider many factors including available budget, gas and electricity tariff, steam availability, and the synergy with other facilities, as well as target supply air conditions.

Above all, the reputation and the field experience of the HVAC vendor or engineering company might be the most important factor affecting the final decision. In the case of a semi-conductor manufacturing factory, for example, the loss caused by stopping production lines for a day due to the failure of humidity control could easily exceed the total benefit of yearly energy saving that might have been otherwise achieved by a new AC system. Therefore, the field engineering at the highest level is required in all life cycle of IAC system.

In this regard, virtual product development (VPD) *via* model based design (MBD) is a promising way to enhance engineering level in a short time at all the phases of product life cycle. In most projects, the experiment at the psychrometric chamber is of limited use unless the field scene is exactly duplicated inside the chamber. Thus, simulations at various levels, from spreadsheet calculation to unsteady CFD, should be performed especially in the early stage to avoid trial and error at the site.

Although AHUs can be customized with high degree of freedom, they are constructed with limited number of elements: duct, fan, condensing unit (CDU), chiller, boiler, coil, desiccant rotor, humidifier, filter, and damper. It is a highly welcome feature for MBD engineers to work with such limited components as building block elements.

A digital mock-up of AHU based IAC system constructed by numerical models of basic elements, can be an economic and, in some sense, superior alternative to partial realization of the real hardware-based system. Since yearly running simulation is possible only in a few hours with the digital mock-up, it can save enormous time and cost for the performance evaluation and control algorithm development. When the digital mock-up interacts with the real asset in the site through sensing data and control algorithm, it is now called a 'digital twin system', which is the main topic of the present paper and is described in the following sections.

2. WORKFLOW TO BUILD A DIGITAL TWIN

Figure 2 illustrates the workflow to build a digital twin and improve the efficiency of the existing AC system by the optimization of the control algorithm. The first step is to collect detailed site information to build a simulator, the virtual system model including AHU components, the outdoor weather data, and the building model of the facility incorporated with the corresponding HVAC load profile.

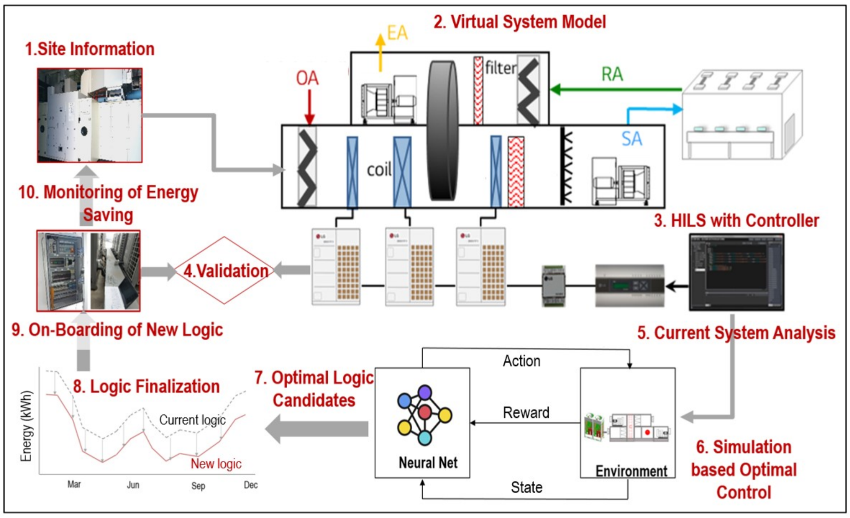

Figure 2: Workflow to build a digital twin AC system and optimal control derivation

Then, DDC, the same controller hardware as the one installed at the site, is connected with a PC at which the simulator is running, building a Hardware-In-the-Loop Simulator (HILS). An accelerated yearly simulation is performed by HILS system adopting the current control algorithm for the evaluation of the system. The operation algorithm of the developed virtual system is then optimized using the reinforcement learning adopting total energy consumption and yearly running cost as the reward. Candidates of optimal logic, or the neural networks obtained as results of the learning are evaluated by yearly running simulation with the HILS system. Finally, the chosen candidate is installed on the DDC as a new operation algorithm at the site. Finally. the energy saving effect of the new algorithm is evaluated by the on-line monitoring system.

3. MAIN COMPONENTS MODELING

3.1 Reference Site Information

Shown in Fig.3 is the schematics on the reference AHU considered in this study, which is one of thirty-one AHUs installed in a battery-separator-film manufacturing factory in Cheong-Ju City, Korea. The AHU operates at nominal air flow rate 250 CMM in order to meet target indoor air condition, 22ºC DB and 25% relative humidity, or 4g/kg humidity ratio. AHU consists of outdoor air duct, regeneration air duct, return air duct, and supply air duct with overall dimension 12.3m (L) x 2.07m (H) x 1.55m (D). A 1.9 m radius-desiccant wheel with Silica Gel as absorbent, is located in the middle of the duct and dehumidifies processing air crossing the lower three quarters of the rotating wheel, while the upper quarter wheel is regenerated by the heated air by a steam coil.

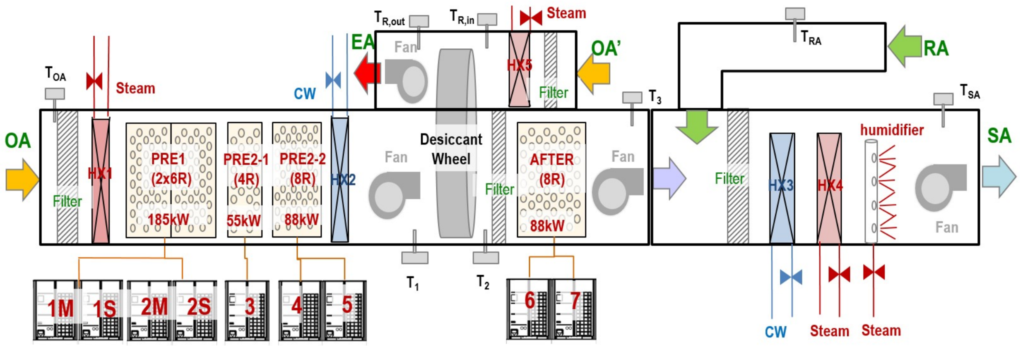

Figure 3: Schematics on the reference site AHU and its components

Numbered outdoor units in Fig. 3 are condensing units for 55~185 kW DX (direct expansion)-cooling coils adopting variable speed scroll compressors to adjust evaporating temperatures depending on the outdoor air condition. CDU-cooling coils are later added to previously chiller-boiler-desiccant driven AHU to reduce the amount of steam supply to regenerate desiccant wheel. Three cooling coils with five CDU's as shown in Fig. 3, are located ahead of desiccant wheel to dehumidify outdoor air as much as possible, while one coil with two CDU's are located behind the wheel to reduce increased dry bulb temperature after the wheel. Total nominal capacity of DX-coil is 402 KW and that of CDU is 513kW.

3.2 Air-Side Simulation for DX-Coil and Duct

It is a common practice to use third-party coils provided by local vendors, which are known to meet designed nominal capacity and pressure drop. This is the case with the DX-coils at the reference site considered in this paper. Since only CAD data for coils are given, additional experiments or simulation should be performed to build numerical models for these coils. Toward this end, air-side large-eddy simulations (LES) are performed for multi-row fin tube heat exchanger with plain fin at various values of frontal velocity yielding pipe-diameter based Reynolds number from 500 to 3500. A second-order accurate, in-house incompressible flow solver (Park and Mahesh 2007) is used for this simulation, which adopts a global coefficient subgrid-scale eddy-viscosity model (Park *et al*. 2006) and immersed boundary method (Kim *et al*. 2001) to handle complex geometry. Fig. 4 shows computed air-side convective heat transfer coefficient and pressure drop compared with those from fins for commercial air-conditioners.

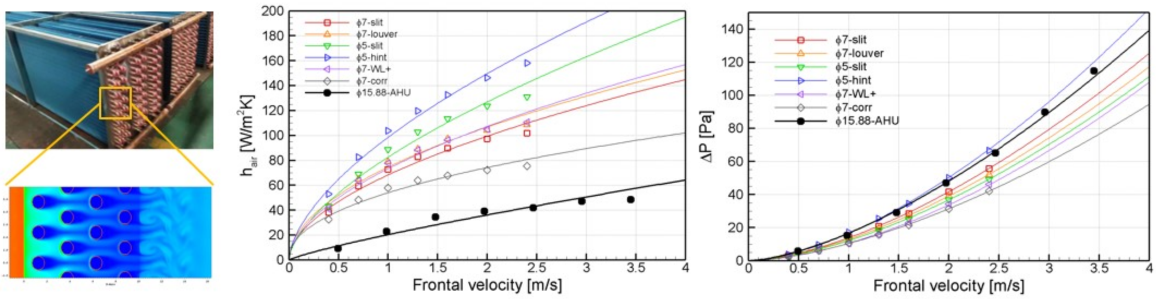

Figure 4: Air-side convective heat transfer coefficient (left) and pressure drop (right) vs. frontal velocity for 4-row evaporator coil with plain fin (denoted as black lines)

Since real time CFD simulation of duct is highly impractical, simulation results as shown Figure 5 at some selected conditions are stored as DB to construct 3D ROM (reduced order model), and they are used in real time calculation. In order to treat fin-tube heat exchanger within affordable grid points, typically several million points, Darcy-Forchheimer porous media model (Mukhopadhyay *et al*. 2012) is used as forcing terms in the momentum and energy equations.

$$\frac{\partial u_i}{\partial t} + \frac{\partial}{\partial x_j}(u_i u_j) = -\frac{\partial p}{\partial x_i} + \frac{1}{Re}\nabla^2 u_i - \frac{u_i}{ReK^*} - \frac{C_f}{\sqrt{K^*}}(u_j u_j)^{1/2} u_i \tag{1}$$

$$\frac{\partial T}{\partial t} + \frac{1}{\sigma}\frac{\partial}{\partial x_j}(u_i T) = \frac{1}{\sigma Re_f Pr_m}\nabla^2 T + \left(\frac{1-\epsilon}{\sigma}\right)\frac{Nu}{Re_f Pr_m \Delta^*}(T_{ref} - T) \tag{2}$$

Here, C_f, K^* are Darcy friction coefficient and permeability, while ε is porosity, σ is the ratio between solid and fluid thermal capacity, and *Nu* is the Nusselt number. They are given from the specification of heat exchanger and results from fin-tube LES mentioned earlier.

As shown in Figure 5, the air velocity profiles across coils are highly non-uniform due to blockage by heat exchangers and bypass area, which implies that simple, uniform flow assumption in heat exchanger simulation might lead to highly inaccurate prediction.

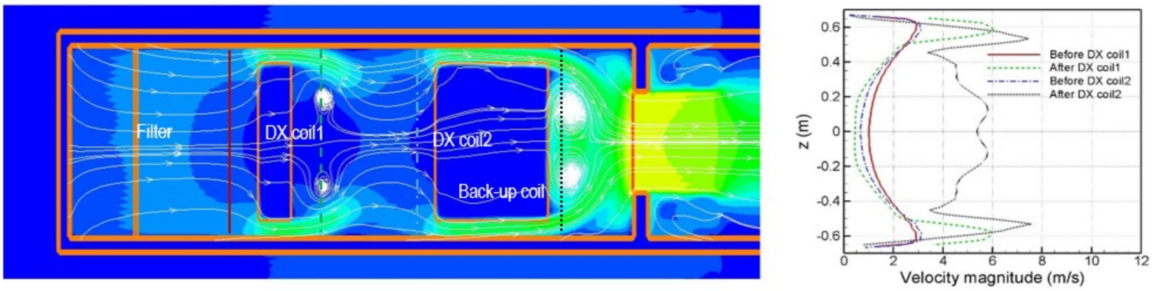

Figure 5: Top-view of the velocity magnitude contour and vectors inside the outdoor air duct (left) and mean velocity profiles at cross sections before and after coils (right)

3.3 DX-Coil with Condensing Unit Model

As described earlier, CDU-DX coil is the key element of the current AHU system adopted to reduce the burden of the desiccant wheel. Thus, all CDUs are operating only in cooling mode while heat pump models are installed at the reference site. The main component of CDU is the variable speed scroll compressor, which is modeled by the geometry based one (Chen *et al*. 2002a, 2002b). Once the compressor speed, suction temperature, suction pressure and discharge pressure are given, discharge mass flow rate and enthalpy are computed by integrating mass and energy equations along the orbiting angle. The model also considers the leakage across the scroll wrap and the vapor injection to increase mass flow rate and decrease discharge temperature.

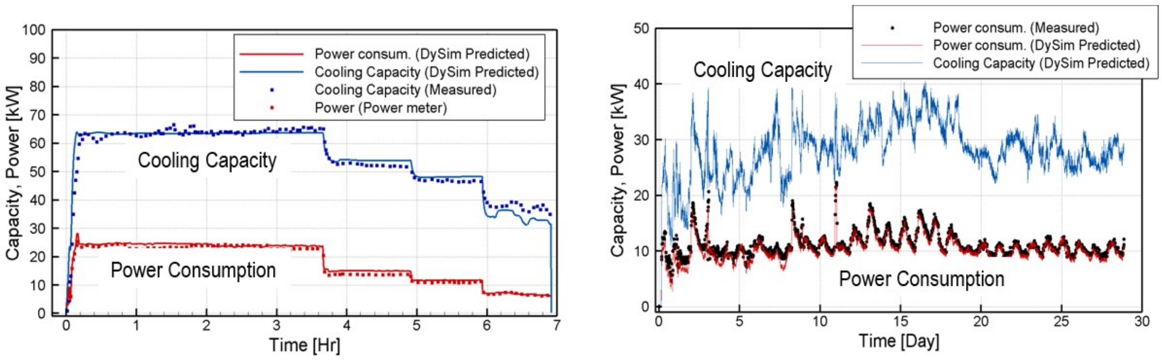

Figure 6: Validation of condensing unit-coil cycle model against chamber data (left) and field measurement (right)

The whole AHU system, however, is too complex for each compressor models to be solved in the above-mentioned manner. Thus, ROM (Reduced Order Model) strategy is again adopted in order to make the computation tractable. In this sense, the stand-alone compressor code is used to create a database for 100,000 points at various points of discharge pressure, suction pressure, suction superheat and compressor speed.

Other components, the outdoor unit condenser, DX-coil, and EEV, are treated in the same way: their performance DB or map-data are created by running their stand-alone codes. Once all DB's for components are given, mass, momentum and energy equations are solved in a quasi-steady manner to determine discharge pressure, suction pressure, and suction enthalpy iteratively. See Park *et al.* (2015) for more details on the solution procedure. Figure 6 shows the validation of the developed cycle code against chamber experiment and the measured data at the reference site. As shown, the model agrees very well with the measured data for both cooling capacity and power consumption within 4% error.

3.4 Desiccant Wheel Modeling

One-dimensional finite-volume model is used for heat and mass transfer across the desiccant wheel considering absorbent characteristics and geometry of the wheel as shown in Fig. 7. See Joos *et al*. (2008) and Bellmo *et al*. (2014) for more details. Also shown in the figure is computed air exit temperature and enthalpy along the rotation direction. It is shown that the model predicts accurate temperature and humidity distribution with temperature and humidity errors ranging 1~5ºC and 0.5~2g/kg.

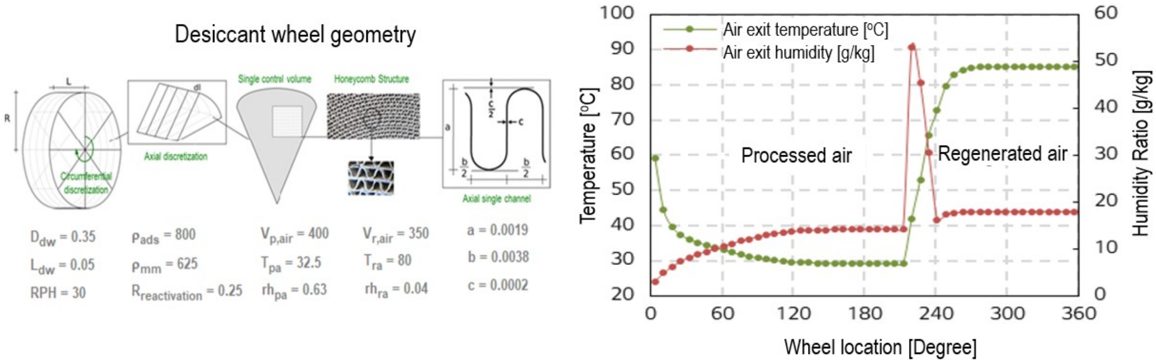

Figure 7: Discretization of desiccant wheel (left) and computed air exit temperature and humidity (right)

3.5 Cooling / Heating Load Calculation

Considering annual operation simulation of AHU, instantaneous HVAC loads at any given instance should be determined together with corresponding outdoor weather data. Figure 8 shows predicted hourly and monthly thermal loads at the reference site based on the standard-year weather data of Cheong Ju City, which are compared with measured data from the outdoor and the return air information at the reference site from January to August, 2021. Here, cooling and heating loads are computed basically by a finite-difference method based on thermal energy balance (Stephenson & Mitalas 1971, Liesen & Pedersen 1997), while the internal heat gain information is obtained from field measurement, or the mean difference between the outdoor air load and the measured total load. As shown in Figure 8. Predicted cooling/heating load agrees well with measured one within 10% error.

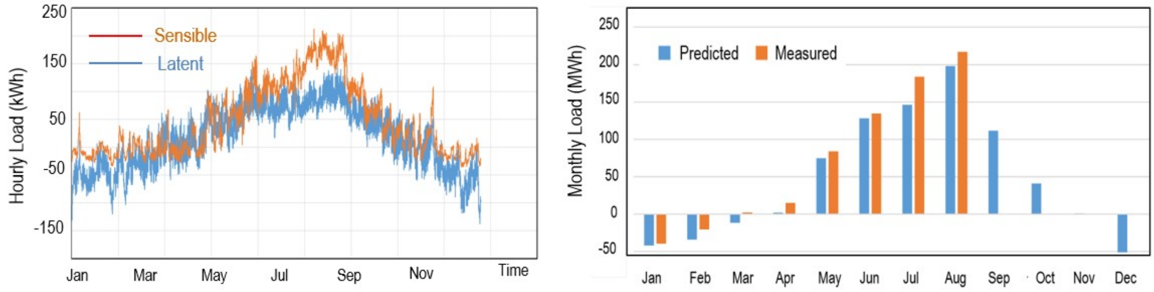

Figure 8: Hourly (left) and monthly (right) thermal loads at the reference site predicted by the load calculation module. Here, negative value denotes heating load.

3.6 Hardware-In-the-Loop Simulation

Figure 9 shown the HILS (Hardware-In-the-Loop Simulation) system used in this study. It is the virtual replica of the reference site in the sense that the same DDC HW and control SW as the ones used in the reference site, interact with numerical models of AHU components including fan, duct, filter, desiccant wheel and coil-CDU. As shown in Figure 9, AHU simulation communicates with DDC, the controller *via* MODBUS (RS-485) protocol in terms of main sensor data such as temperature, humidity, air flow rate and actuator values, which are then monitored by a dedicated monitoring SW at a remote cloud server. A Python code built on the DDC HW and OS system, as the main controller SW, exclusively handles all the devices and actuators based on the sensing data.,

Using this HILS system, one can easily test and modify control algorithm and/or HW specifications to predict how these changes affect supply air and energy consumption without trial and error at the site. Now, we are ready for simulation-based optimization of the system, which will be discussed in the subsequent section.

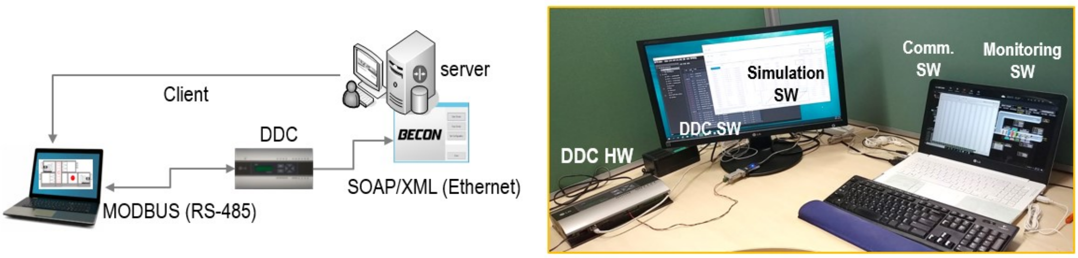

Figure 9: Hardware-In-the-Loop Simulation of AHU system with controller HW

4. CONTROL ALGORITHM OPTIMIZATION

In this section, the optimal control algorithm for determining target refrigerant temperatures of CDUs, is proposed using virtual AHU solution mentioned in the earlier sections. Figure 10 shows the model optimization framework by reinforcement learning for the pressure target vector. Since the target refrigerant pressure is continuous parameter, it is strongly required to digitize its value to make the optimization problem tractable. In this sense, the target pressure of the refrigerant R410A, ranging from 500 kPa to 1100 kPa, is digitized into 11 values from 0 to 10, where 0 denotes compressor OFF mode, as shown in Figure 10. Then, the target pressure vector in Fig. 10, for example, is $Pe_{targ} = (1,3,6,0,0)$.

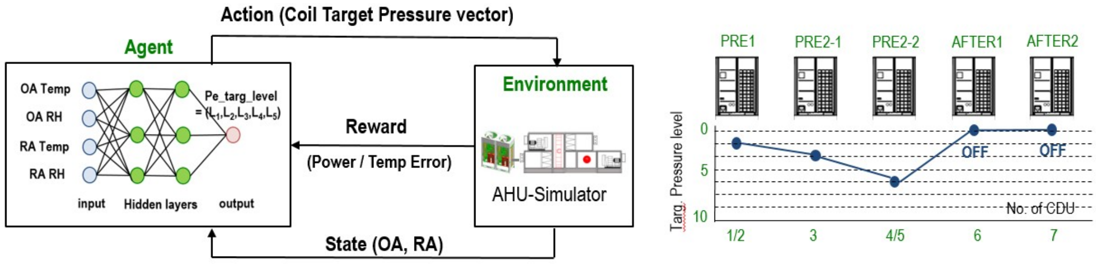

Figure 10: Model optimization framework by reinforcement learning (left) and the illustration of the optimal pressure target vector (right)

Our goal is to obtain the agent, or the neural network, to compute Pe_{targ} for given state, or the outdoor air temperature, outdoor air relative humidity, return air temperature and humidity. To this end, a Deep Q-learning, or DQN algorithm (Minh *et al*. 2013; Minh *et al*. 2015) is applied. Here, 'reward' is defined as the total power consumption from all the devices divided by temperature error, or the deviation from target DB and WB temperatures.

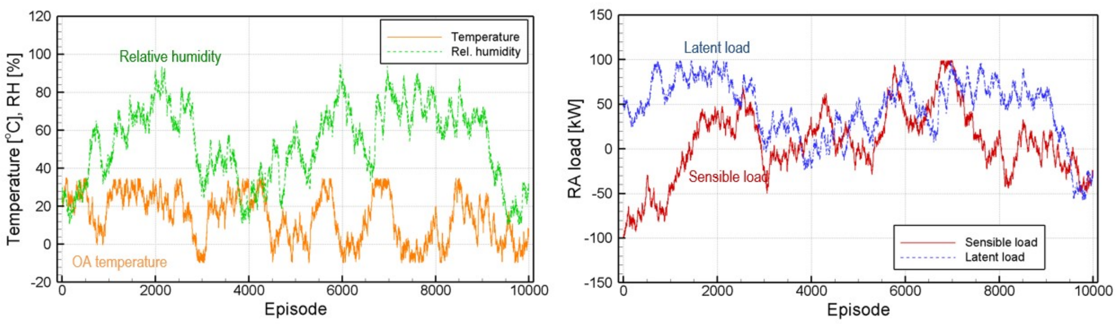

Figure 11: Random episode generation for reinforcement learning: Outdoor air temperature and relative humidity (left), sensible and latent thermal load from return air (right)

Since the reinforcement learning should be performed at continuously new states, or OA/RA conditions, total 10,000 random episodes following the Weiner process are generated as new states as shown in Figure 11. Generated episodes covers all possible weather and return air conditions that might occur at the reference site. Each episode is assumed to be one-hour weather and return-air condition: developed AHU-simulator is solved for given one hour at fixed condition and returns a new reward and state as the output. Then, the weights of agent neural network is updated according to reward value. The final neural network after the completion of all learning episodes is realized in DDC in the form of a new control algorithm written in Python language, which will replace the current rule-based one.

Figure 12 shows predicted monthly electricity and gas energy consumption and corresponding operation costs depending on the control algorithms adopted. The current rule-based operation algorithm relies only on the outdoor air humidity ratio to determine target evaporating pressures for CDU, while the optimal algorithm adopts the inference value from the neural network determined by DQN algorithm described above. It is shown that the optimal logic can save 70.8% of gas energy consumption minimizing the steam amount for the regeneration of the desiccant wheel, while it can save 17.2% of electricity consumption mainly in the cooling season yielding 53.7% total energy saving. The energy cost saving from the optimal logic is 45.6% which amounts to 63,000 USD per year yielding 2.9 year payback period for CDU-DX coil introduction.

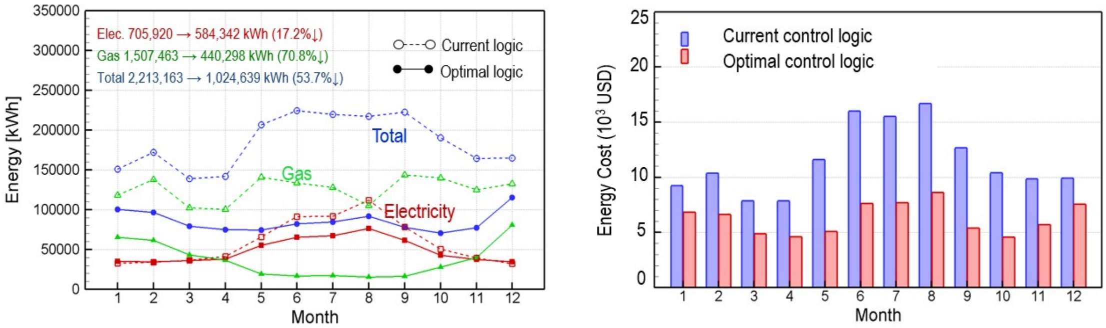

Figure 12: Comparison of monthly electricity and gas consumption (left) and energy cost (right) between the current and the optimal control algorithm

In order to see how the optimal algorithm for CDU affects other components and the overall AHU system, a psychrometric chart obtained from the new algorithm is compared with that from the current algorithm as shown in Figure 13. A randomly chosen time instance is 14:00, July 25th, which belongs to a typical cooling dominated season. At this instance, the outdoor air condition is 25°C DB and 14 g/kg. Having the same target supply air condition, or 22°C DB and 4g/kg, two algorithms choose completely different paths to reach the target. It is clear that the optimal algorithm, unlike the current one, tries to take the nearest possible shortcut to the target avoiding overcooling and overheating. As a result, the new algorithm achieves 78% savings in steam usage to regenerate the desiccant wheel and total 45% energy saving. Although not shown here, investigations at other instances results in similar conclusions, which clearly explains huge yearly energy saving in Figure 12.

5. CONCLUSIONS

In this study, we introduced the model-based design (MBD) of air-handling unit (AHU) based industrial air conditioning system and its optimal control strategy by machine learning. This study shows the feasibility of MBD solution contributing to the all stages of the industrial air-conditioning business: In the proposal stage, a report based on realistic simulation can help predicting whether the current devices can fulfill the desired supply air condition. In the maintenance stage, the control algorithm optimization can help minimizing the running cost. In this sense, MBD can be extended to be a digital twin system that can upgrade the physical asset as shown in Figure 14.

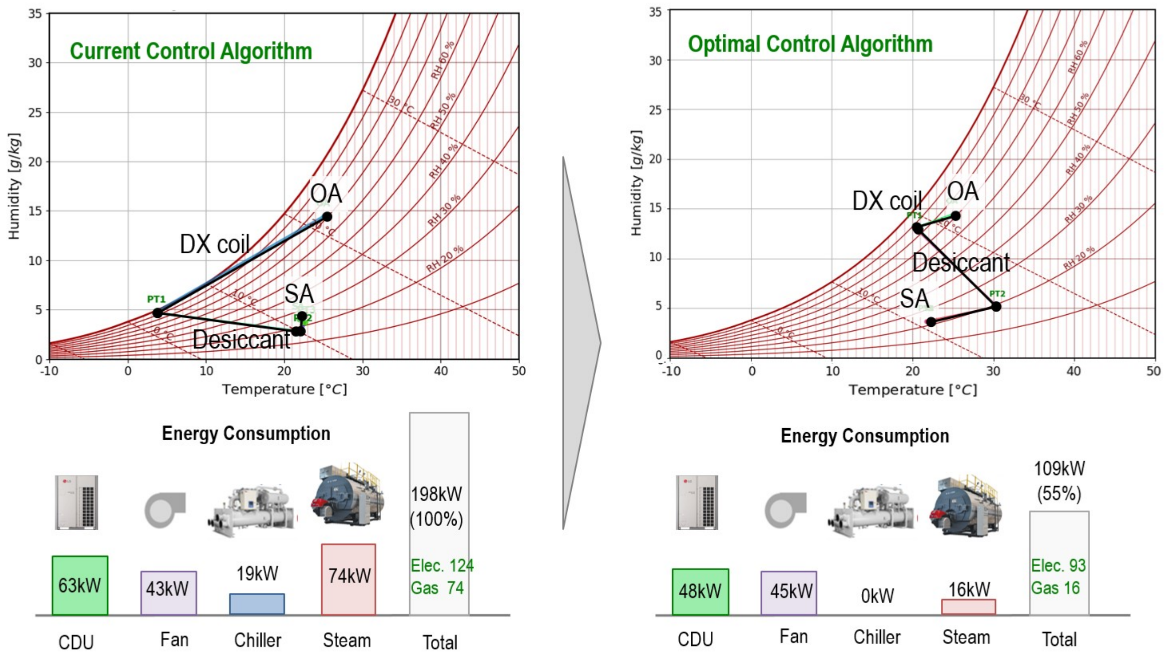

Figure 13: Comparison of the psychrometric chart and energy consumption at a randomly chosen instance at the reference site with the current and the optimal control algorithm

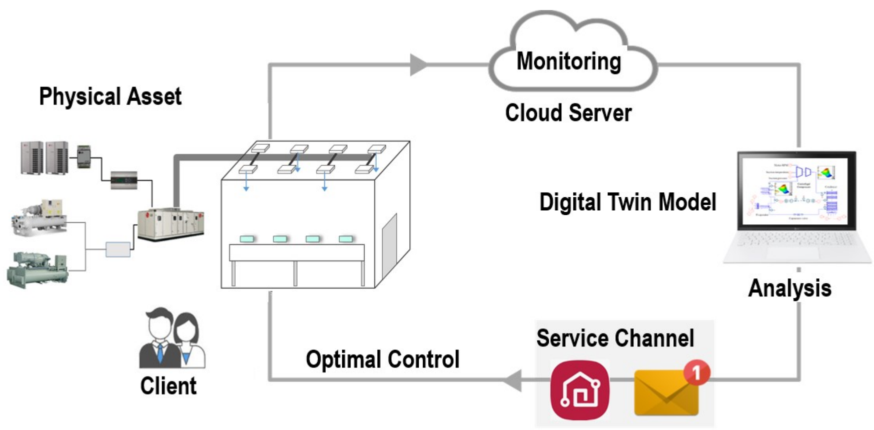

Figure 14: On-line care service based on a digital twin model

REFERENCES

Bellemo, L., Elmegaard, B., Kærn, M. R., Markussen, W. B., Reinholdt, L. O. (2014). Steady state modeling of desiccant wheels, *Proceedings of the International Sorption Heat Pump Conference*, ISBN 978-1-63266-596-6

Chen, Y., Halm, N. P., Groll, E. A., & Braun, J. E. (2002). Mathematical modeling of scroll compressors-part I: compression process modeling. *Int. J. Refrig.*, Vol. 25(6), 731–750.

Chen, Y., Halm, N. P., Braun, J. E., & Groll, E. A. (2002). Mathematical modeling of scroll compressors-part II: overall scroll compressor modeling. *Int. J. Refrig.*, Vol. 25(6), 751–764

Joos, A., Schmitz, G., Casas W. (2008). Enhancement of a Modelica model of a desiccant wheel, *Modelica 2008*, Mar. 3-4, 2008.

Kim, J, Kim, D, Choi, H (2001). An Immersed-boundary finite-volume method for simulations of flow in complex geometries, *J. Comp. Phys*., Vol. 171(1),, 132-150.

Liesen, R.J., Pedersen, G. O. (1997). An evaluation of inside surface heat balance models for cooling load calculations. *ASHRAE Trans.* 103(2):485-502.

Minh, V., Kavukcuoglu, K., Silver, D., Graves, A., Antonoglou, I., Wierstra, D., Riedmiller, D. (2013) Playing Atari with Deep Reinforcement Learning, *arXiv*: 1312.5602v1 [cs:LG]

Minh. V., Kavukcuoglu, K., Silver, D., Rusu, A. A., Veness, J., Bellemare, M. G., Graves, A., Riedmiller, D, Fidjeland, A. K., Ostrovski, G., Petersen, S., Beattie, C., Sadik, A., Antonoflou, I. King, H., Kumaran, D., Wierstra, D., Legg, S., Hassabis, D. (2015), Human-level control through deep reinforcement learning, *Nature*, Vol. 518, 529-533.

Mukhopadhyay, S., De, P. R., Bhattachayya, K. (2012). Forced convective flow and heat transfer over a porous plate in a Darcy-Forchheimer porous medium in presence of radiation, *Meccanica*, vol. 47, 153-161.

Park, N., Lee, S., Lee, J., Choi, H. (2006). A dynamic subgrid-scale eddy viscosity model with a global model coefficient, *Phys. Fluids*, Vol. 18, 125109

Park, N., Mahesh, K. (2007). Numerical and modeling issues in LES of compressible turbulence on unstructured grids, *AIAA 2007-722*, 45th AIAA Aerospace Science Meeting and Exhibit, Jan. 8-11, Reno, Nevada, USA

Park, N., Shin, J., Chung, B., Kim, B. (2015). A new dynamic heat pump simulation including frosting and defrosting models, *Trans. KSME C: Technology and Education*, Vol. 3(1), pp. 1~13

Stephenson, D.G., Mitalas, G.P. (1971). Calculation of heat transfer functions for multi-layer slabs. *ASHRAE Trans.* 77(2):117-126.

.